Jurnal Tribologi 23 (2019) 125-136

MYTRIBOS Malaysian Tribology Society
Jurnal Tribologi
Website : jurnaltribologi.mytribos.org e-issn: 2289-7232

Investigation of cutting forces in end milling of AISI 4340 under dry and cryogenic conditions

Shalina Sheik Muhamad [1,*], Jaharah A. Ghani [1], Che Hassan Che Haron [1], Hafizal Yazid [2]

[1] Fakulti Kejuruteraan dan Alam Bina, Universiti Kebangsaan Malaysia, 43600 Bangi, Selangor, MALAYSIA.
[2] Agensi Nuklear Malaysia, Bangi, 43000 Kajang, Selangor, MALAYSIA.
*Corresponding author: P91996@siswa.ukm.edu.my

KEYWORDS

AISI 4340
End mill
Cutting force
Dry and cryogenic
Taguchi method

ABSTRACT

This paper presents the effects of cutting parameters on the cutting force when machining AISI 4340 steel in a dry and cryogenic environment. Taguchi was used in the design of the experiment and analysis of variance (ANOVA) was employed to identify the percentage of contributions among the four cutting parameters (cutting speed, feed rate, axial depth of cut and radial depth of cut) to the cutting force. The indexable carbide insert type of end mill with downmill approach was used in this experiment using a straight line machining strategy. The forces were measured using a custom made strain gauge force dynamometer at the UKM. The results showed that the radial depth of cut was the dominating factor exerted on cutting force, followed by speed and feed rate, for both cutting environments. The experiment showed that the cryogenic application was able to reduce the cutting force by up to 39 % when compared to dry machining. The cryogenic LN effect efficiently reduced the cutting temperature at the cutting point which is believed to be the main factor contributing to an improvement in cutting force.

1.0 INTRODUCTION

The AISI 4340 medium carbon high strength low alloy steel is mostly used in the automotive and machine tool industries. It is a low alloy steel containing nickel, chromium, and molybdenum. Among the various applications are its use in high strength machine parts, bearings, gears, shafts,

Received 16 October 2019; received in revised form 18 November 2019; accepted 2 December 2019.
To cite this article: Muhamad et al. (2019). Investigation of cutting forces in end milling of AISI 4340 under dry and cryogenic conditions. Jurnal Tribologi 23, pp.125-136.

and cams, which require tighter geometric tolerances, longer service life, and good surface finish (Agrawal et al., 2015). The typical yield strength and hardness ranges of AISI 4340 are from 470 MPa (annealed) to 1725 MPa (quenched and tempered) and 17 to 49 HRC respectively (Al-Ghamdi et al., 2015).

Cutting force is an important factor in machining operations as it strongly influences the cutting temperature, tool wear, and others. The analysis of the cutting forces provides an understanding of the mechanics of machining. The cutting forces data is crucial for minimizing distortion of machine components, avoiding excessive distortion of workpiece, fixture or cutters, and selecting an appropriate machine tool with suitable power (Qian & Hossan, 2007). The cutting forces of milling are cyclic, and normally, the peak forces are the most important values because these can be used to establish appropriate dimensions in the machine-tool or in the cutting tool design (Gonzalo et al., 2010). It also the main contributor in determining the energy consumed and machining power required for the process, tool and workpiece deflections (Kosaraju et al., 2012).

The Taguchi method or technique has been widely used in engineering methodology for improving productivity. Most of the investigations using Taguchi techniques have used orthogonal arrays and signal-to-noise (*S/N*) ratio analysis in order to determine the optimal values of cutting parameters which minimizes the response variable. Analysis of variance (ANOVA) is the statistical method used to interpret experimental data. It detects any differences in the average performance of groups of items tested (Camposeco-Negrete, 2013). There have been many recent applications of Taguchi techniques for investigating machinability, process optimization and for optimizing power consumption.

In the work of Khare & Agarwal, (2017) , the Taguchi technique was applied to modelling and was used to optimize the machining parameters (cutting speed, feed rate, depth of cut and rake angle) for minimum surface roughness on AISI 4340 steel. The machining operations were performed under cryogenic condition. An orthogonal array and *S/N* ratio were employed to analyze the effects of cutting parameters on the surface roughness. Qasim et al., (2015) utilized Finite Element (FE) simulations to investigate the effects of varying cutting speed, feed rate, depth of cut, and rake angle in the orthogonal cutting process of AISI 1045 steel. The cutting parameters were optimized by multi-response considerations namely cutting forces and temperature. Taguchi matrix, (S/N) ratio, and ANOVA were used to find the optimum values of cutting parameters which could minimize cutting forces and temperature. The results showed that for optimum cutting forces, feed rate and depth of cut are the most important factors while for lower temperatures, cutting speed and rake angle have significant effects.

Cryogenic machining, as an alternative approach to the conventional cooling approach, has been accepted in terms of its competitive advantages. In cryogenic machining applications, liquid nitrogen has frequently been used as a cryogen. As claimed by Muhamad et al., (2019) this strategy could be used to reduce the average surface roughness of the machined part. Moreover, Musfirah et al., (2017) claimed that the application of liquid nitrogen could reduce tool wear, lower the required cutting force and eliminate contamination of the machined part. Ahmed & Hrairi, (2012) measured and compared the tool wear and surface roughness of dry conditions with the cryogenic turning of AISI 4340 steel. They found out that use of cryogenic cooling at high depths of cut, high feed values and high cutting speeds resulted in decreases in tool wear and surface roughness. However, using cryogenic cooling at low speeds, small feed and depths of cut would not result in any prominent effect. Kaynak & Gharibi, (2018) conducted turning experiments under dry, LN, CO2 and CO2 conditions with MQL on tool wear of AISI 4140 steel using uncoated carbide tools. The results revealed that carbon dioxide-assisted cryogenic machining leads to the largest occurrence of flank and nose wear, in comparison with dry and liquid nitrogen-assisted machining. The use of liquid nitrogen-assisted cryogenic machining results in a reduction of tool flank and nose wear.

The cutting forces in cryogenic machining depend on material properties and the cooling method. Cryogenic coolant could increase the strength and hardness of tool or workpiece materials (Singla et al., 2018). The hardness of the material could have increased due to work hardening and grain refinement from cryogenic machining, where both of these depend on the type of work material. In general, materials with a face-centered cubic (fcc) lattice keep their ductility at cryogenic temperatures, whereas body-centered cubic (bcc) and hexagonal-closed packed (hcp) materials become brittle (Jawahir et al., 2016). There are three methods for cooling by using a cryogen in machining. These methods are: cooling at the cutting region, workpiece cooling and indirect cooling of the cutting tool (Muhamad et al., 2018). A combination of these methods can also be used. The method of cooling at the cutting region enhances machinability, enhances cutting tool properties and modifies the properties of the workpiece. However, using an appropriate flow rate of the cryogenic coolant is very crucial in reducing the coefficient of friction and also to avoid excessive cooling of the workpiece which can cause work hardening (Deshpande et al., 2018). Work hardening increases the cutting forces and the friction forces at the contact between the workpiece and cutting tool edge (Zhong et al., 2018).

This paper presents experimental work in milling of AISI 4340 using PVD coated TiAlN and AlCrN carbide tools with various parameters. The cutting force was measured experimentally using a dynamometer under dry and cryogenic conditions. The Taguchi design of the experiment was selected to find the relationships between the control parameters. The cutting speed (v_c), the feed rate (f_z), the axial depth of cut (a_p) and radial depth of cut (a_e) were taken as control factors. This study was intended to compare the cutting force of a cryogenic application with a dry environment in the end milling of AISI 4340 alloy steel.

2.0 EXPERIMENTAL PROCEDURE

In this study, Taguchi techniques were employed using orthogonal arrays, *S/N* ratio analysis and ANOVA to find the optimal values of process parameters. This method allowed fewer experimental runs for obtaining results. *S/N* ratios used in the present study were smaller which were better characteristics because the purpose of the experiment was to find values which minimized cutting force. The *S/N* ratio was calculated as in Equation (1)

$$\frac{S}{N} = -10 * \text{Log}(\frac{1}{n}) \sum_{i-1}^{n} \frac{1}{{y_i}^2} \quad (1)$$

Where y_i is the observed data and n is the number of observations. The optimal level of the process parameters is the level with the highest *S/N* value. ANOVA was performed to study the contribution of the factors and to explore the effects of each factor on the observed values (Md Radzi et al., 2018). Main effects plots allowed identification of the level of each factor which provided the minimum response value (Camposeco-Negrete, 2013).

The set-up parameters were based on the machine capability, tools manufacturer's catalogues and previous research by Natasha et al., (2018). The cutting parameters for this study were as shown in Table 1. The selected variables viz. cutting speed, feed rate, axial depth of cut and radial depth of cut and three levels have been considered. According to the array selector given by Tan et al., (2017), if there are 4 parameters and 3 levels of each, the Taguchi L9(3^4) array is sufficient to optimize the parameters. Nine sets of experimental combinations for each condition were generated using Taguchi L9 design of experiments, as shown in table 2. An appropriate orthogonal array was selected to analyze the effects of these parameters on cutting forces.

Milling experiments were performed on 165 mm x 100 mm x 100 mm dimension of AISI 4340 steel piece with an average hardness of 32 HRC. The experimental investigation was carried out on a DMG-ECO vertical milling machine, with a maximum spindle speed of 8000 RPM. The cutting tool and tool holder specifications are shown in Table 3. The number of indexable carbide inserts of the cutter was 3. But only one insert was used for machining in this present study in order to avoid the tooltip run-out on tool wear analysis. For each experiment, a fresh cutting edge was used. In dry machining, the experiments were performed without use of any cooling liquid. In the cryogenic machining process, LN at -197°C was applied to the cutting zone via a nozzle. Liquid nitrogen under 2 MPa pressure and approximately 1.159 x 10^{-3} m^3/s flow rate was set to ensure no excessive cooling. The cryogenic delivery setup was based on previous research by Natasha et al., (2016). Figure 1 shows the complete setup assembly used for the milling experiments.

Table 1: Cutting parameters and their levels.

Cutting parameters	**Level 1**	**Level 2**	**Level 3**
v_c: Cutting speed	200	250	300
f_z: Feed rate	0.15	0.20	0.30
a_p: Axial depth of cut	0.3	0.4	0.5
a_e: Radial depth of cut	0.20	0.35	0.50

Table 2: L9 Orthogonal Array design of experiments.

Exp. No.	**v_c (m/min)**	**f_z (mm/tooth)**	**a_p (mm)**	**a_e (mm)**
1	200	0.15	0.3	0.20
2	200	0.20	0.4	0.35
3	200	0.30	0.5	0.50
4	250	0.15	0.5	0.35
5	250	0.20	0.3	0.50
6	250	0.30	0.4	0.20
7	300	0.15	0.4	0.50
8	300	0.20	0.5	0.20
9	300	0.30	0.3	0.35

Table 3: Cutting tool and inserts specifications (Sumitomo, 2017)

Items	**Value**
Number of teeth	3
Tool diameter	20 mm
Thickness of cutting insert	3.58 mm
Rake angle	28°
Clearance angle	11°
Coating	TiAlN /AlCrN

The cutting forces in both conditions were measured by dynamometer during machining. The dynamometer was a custom made strain gauge force dynamometer at the UKM mounted on a machine table. The work piece was mounted on a dynamometer linked to an acquisition data system in order to measure the force during milling. The output of the dynamic cutting force signal was observed in real time, stored, and displayed by a GUI software known as NeoMoMac software. The cutting forces were measured at the beginning of the cut for both cutting conditions, to disregard the tool wear.

The force signal acting on this dynamometer was measured in three directions, namely feed force (F_x), normal force (F_y), and axial force (F_z). The resultant force, F_R, consisting of F_x, F_y, and F_z, which are associated with forces in the x, y and z-direction, respectively. F_R acting on the cutter can be calculated as given in Equation (2) (Alauddin et al., 1996).

$$F_R = \sqrt{{F_x}^2 + {F_y}^2 + {F_z}^2} \quad (2)$$

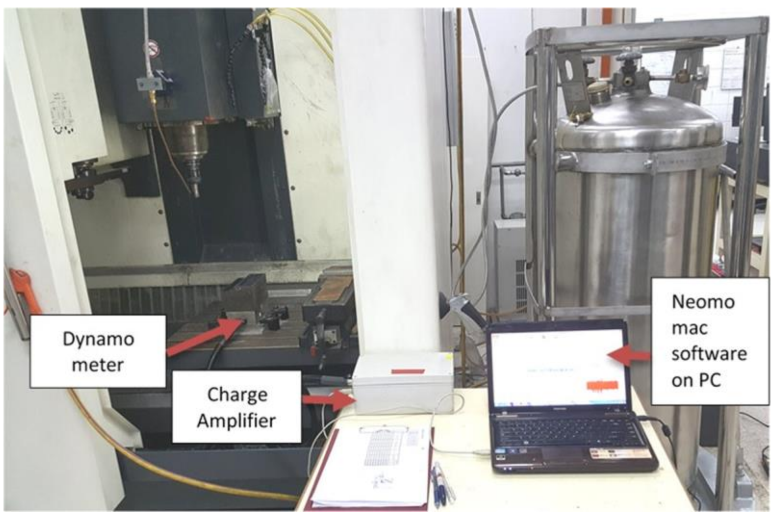

Figure 1: Experimental setup for milling tests with cryogenic cooling systems.

3.0 RESULTS AND DISCUSSION

The components of the cutting force shown in Figure 2 were obtained from experiment no 9 in dry condition during the 5 passes of run. The cutting forces were analyzed by programs or algorithms using Matlab software which analyses all the signals during the machining. Large amplitude of F_z at the beginning of each machining pass, indicated that there was vibration and tool deformation in this direction. The resultant force for both conditions were as shown in Table 4. From the exprimental results, the resultant force achieved was in the range of 204 N to 407 N under both cutting conditions. Almost similar findings were reported in previous work on machining of AISI 4340. For example, 421.43 N machining force obtained at the cutting speed of 147 m/min, feed rate 0.10 mm/rev and depth of cut 0.6 mm with multilayer CVD coated (TiN/TiCN/Al_2O_3) carbide inserts at 49 HRC by Das et al., (2014); and 264 N machining force obtained at the cutting speed of 150 m/min, feed rate 0.18 mm/rev and depth of cut 0.2 mm with TiN coated carbide inserts at 47 HRC by Sahoo & Sahoo, (2012). Both experiments were conducted under dry conditions.

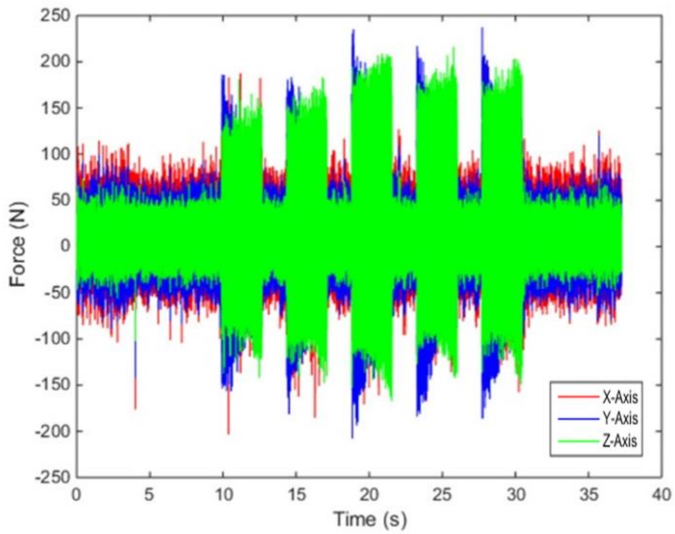

Figure 2: Cutting forces components in x, y and z-axis.

Table 4: Resultant force under different cutting parameters.

Exp. No.	F_R (N) (Dry)	F_R (N) (Cryogenic)
1	264.69	212.67
2	329.04	280.44
3	405.54	364.48
4	214.19	206.53
5	323.90	239.40
6	288.95	203.64
7	407.04	248.49
8	284.91	210.34
9	320.45	279.20

The main effects analysis was used to study the trend of the effects of each of the factors. Main effects plot for the four factors considered (cutting speed, axial depth of cut, radial depth of cut and feed rate) have been shown in Figure 3 and 4 for dry and cryogenic cooling respectively. The figures reveal that cutting speed, feed rate, and radial depth of cut significantly affect the machining forces. This result is in line with the study carried out by Das et al., (2016). It was also observed that the axial depth of cut was not significant on the exerted force. Therefore, this non-significant cutting parameter was removed. In Figures 3 and 4, force increased with the increase in feed rate. The increase in feed rate increased the chip thickness as the forces were in proportion with the chip area as mentioned in Subramanian et al., (2013). This is in line with (Jebaraj & Pradeep Kumar, 2019) who surmised that the increase in feed rate resulted in an increase in the area of the shear planes to the cutting forces.

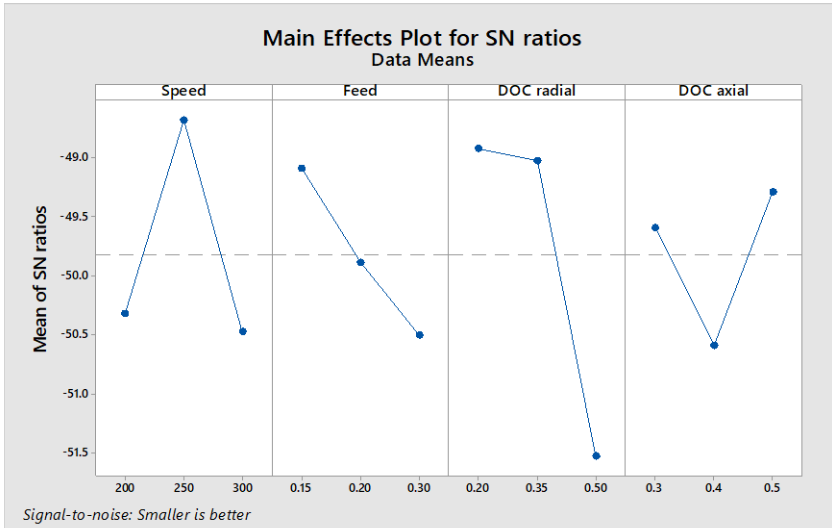

Figure 3: Main effect plot for resultant force under dry conditions.

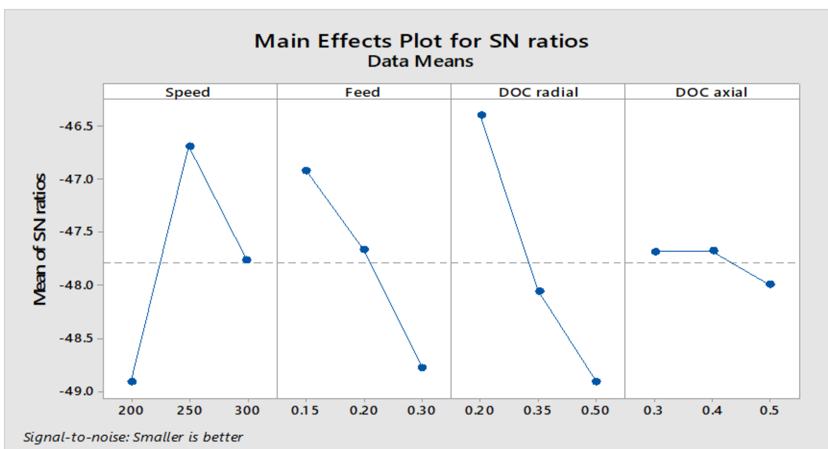

Figure 4: Main effect plot for resultant force under cryogenic conditions.

It also revealed that cutting force increased with the increase of radial depth of cut. According to the work of Kasim et al., (2013), it was stated that the feed rate and radial depth of cut plays an important role on cutting forces. This could be described with reference to Figure 5, which is the representation of the cutting tool model. When the radial depth of cut affects the tangential angle, γ in conjunction with the tangential force, f_t. The engaged angle, λ was influenced by the combination of feed rate and radial depth of cut. During tool rotation, it may increase the radial depth of cut and increase the contact area. It was correlated with the thickness of the chip.

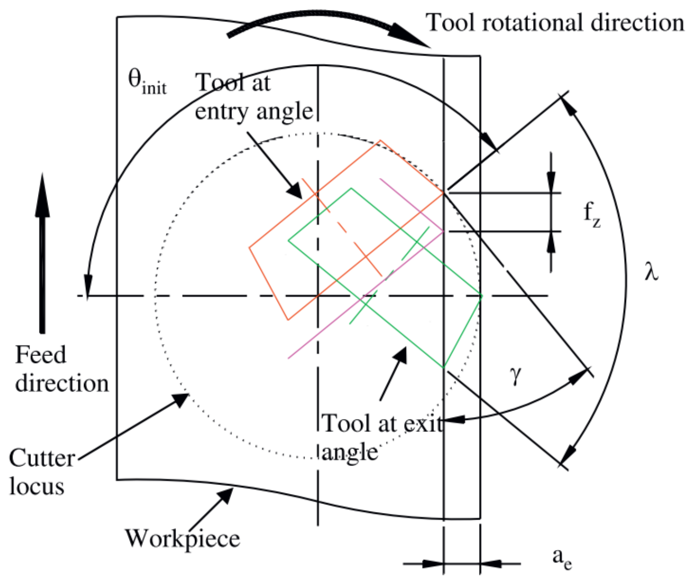

Figure 5: Top view of peripheral milling indicates the nomenclature related to the development of the model. Adapted after (Kasim et al., 2013).

Tables 5 and 6 show the results of ANOVA for resultant force under both conditions. It can be found that cutting speed and radial depth of cut are significant cutting parameters affecting resultant force. The order of contribution of the cutting parameters affecting force is the radial depth of cut, cutting speed and feed rate under both conditions. Therefore, based on the S/N and ANOVA analyses, the optimal cutting parameters for minimum resultant force is low cutting speed, low feed rate and low radial depth of cut under both conditions.

Table 5: ANOVA- resultant force under dry cutting condition.

Parameter	DF	Seq SS	Contribution	Adj MS	F-Value	P-Value
v_c	2	7133	22.82%	3566	2.3	0.303
f_z	2	2810	8.99%	1405	0.9	0.525
a_e	2	18200	58.24%	9100	5.86	0.146
Error	2	3108	9.94%	1554		
Total	8	31251	100.00%			

Table 6: ANOVA- resultant force under cryogenic cutting condition.

Parameter	DF	Seq SS	Contribution	Adj MS	F-Value	P-Value
v_c	2	7265.5	33.02%	3632.7	13.37	0.07
f_z	2	5543.2	25.19%	2771.6	10.2	0.089
a_e	2	8649.7	39.31%	4324.8	15.92	0.059
Error	2	543.3	2.47%	271.7		
Total	8	22001.7	100.00%			

From Figure 6, the resultant force obtained in machining with cryogenic coolant was found to be lower to those obtained in dry machining. Results indicate that cryogenic machining was able to reduce the resultant force up to 39 % percent compared to the dry machining. This have been due to the application of LN which reduces the chip-tool contact length, break-in wear at the cutting edges and close-curling of the chips, which leads to reduction in the cutting forces (Dhar & Khan, 2006). Previous researchers (Ke et al., 2009; Ravi & Pradeep Kumar, 2011) have also proven that the application of LN enhances chip flow and reduces the coefficient of friction in the interface of the tool and chip, which leads to lower cutting forces than those observed in dry machining. Cryogenic coolant reduced the welding tendency and temperature, but it could also increase the hardness of the tool or workpiece material (Kaynak & Gharibi, 2018). In cryogenic machining, the cutting forces depend on the material properties and the cooling method (Jebaraj & Pradeep Kumar, 2019). Since the LN was sprayed directly on the cutting tool instead on the workpiece and there was no excessive cooling to the workpiece, cryogenic cooling showed significant improvement in relation to the cutting forces.

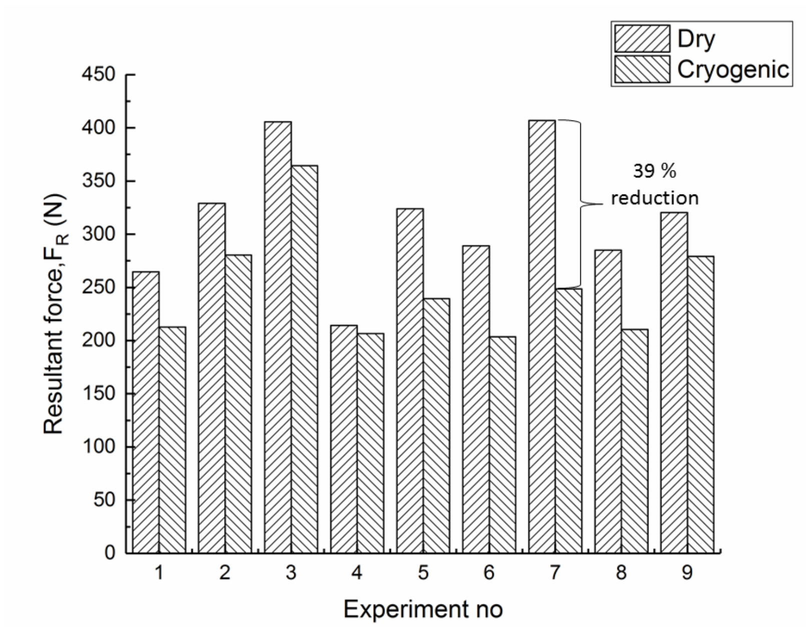

Figure 6: Resultant force for various cutting speeds and feed rate.

4.0 CONCLUSION

This paper has discussed an application of the Taguchi method to show the relationship between cutting parameters and cutting force during end milling operations of AISI 4340. Resultant force for both cryogenic and dry cutting conditions were compared experimentally. The following can be concluded:

(a) For minimizing the force generated, the radial depth of cut is the most significant factor under both conditions.

(b) The minimum force was obtained when the cutting speed was set at 200 m/min, radial depth of cut of 0.2 mm, axial depth of cut of 0.3 mm and feed rate of 0.15 mm/tooth under cryogenic cooling condition.
(c) The experiment results indicate that the cryogenic application is able to reduce cutting force up to 39 %, compared to dry milling.
(d) From this work, it has been shown that it is possible to control the machining parameters to achieve the desired cutting force and it is also possible to estimate the power requirement in machining of AISI 4340 steel.
(e) The work hardening effect in machinability and surface integrity will be studied in future work involving FEM simulation, microstructure, and phase changes during the dry and cryogenic machining processes.

ACKNOWLEDGEMENT

The authors would like to thank the Universiti Kebangsaan Malaysia (UKM) for their financial support under a DIP-2018-026 and GUP-2017-048 Grants.

REFERENCES

Agrawal, A., Goel, S., Rashid, W. B., & Price, M. (2015). Prediction of surface roughness during hard turning of AISI 4340 steel (69 HRC). Applied Soft Computing, 30, 279-286.

Ahmed, M. I., & Hrairi, M. (2012). Efficient Cryogenic Cooling during Machining of Rolled AlSl 4340 Steel. In Advanced Materials Research (Vol. 576, pp. 123-126). Trans Tech Publications.

Al-Ghamdi, K. A., Iqbal, A., & Hussain, G. (2015). Machinability comparison of AISI 4340 and Ti-6Al-4V under cryogenic and hybrid cooling environments: a knowledge engineering approach. Proceedings of the Institution of Mechanical Engineers, Part B: Journal of Engineering Manufacture, 229(12), 2144-2164.

Alauddin, M., El Baradie, M. A., & Hashmi, M. S. J. (1996). Modelling of cutting force in end milling Inconel 718. Journal of Materials Processing Technology, 58(1), 100-108.

Camposeco-Negrete, C. (2013). Optimization of cutting parameters for minimizing energy consumption in turning of AISI 6061 T6 using Taguchi methodology and ANOVA. Journal of Cleaner Production, 53, 195-203.

Das, A., Mukhopadhyay, A., Patel, S. K., & Biswal, B. B. (2016). Comparative assessment on machinability aspects of AISI 4340 alloy steel using uncoated carbide and coated cermet inserts during hard turning. Arabian Journal for Science and Engineering, 41(11), 4531-4552.

Das, S. R., Nayak, R. P., Dhupal, D., & Kumar, A. (2014). Surface Roughness, Machining Force and FlankWear in Turning of Hardened AISI 4340 Steel with Coated Carbide Insert: Cutting Parameters Effects. International Journal of Automotive Engineering, 4(3), 758-768.

Deshpande, Y. V., Andhare, A. B., & Padole, P. M. (2018). How cryogenic techniques help in machining of nickel alloys? A review. Machining Science and Technology, 22(4), 543-584.

Dhar, N. R., & Khan, M. M. A. (2006). An Experimental Study of Cryogenic Cooling Effects in Machining AISI-4140 Steel. Journal of Engineering and Technology, 5(2), 21–35.

Gonzalo, O., Beristain, J., Jauregi, H., & Sanz, C. (2010). A method for the identification of the specific force coefficients for mechanistic milling simulation. International Journal of Machine Tools and Manufacture, 50(9), 765-774.

Huang, X., Zhang, X., Mou, H., Zhang, X., & Ding, H. (2014). The influence of cryogenic cooling on milling stability. Journal of Materials Processing Technology, 214(12), 3169-3178.
Jawahir, I. S., Attia, H., Biermann, D., Duflou, J., Klocke, F., Meyer, D., ... & Schulze, V. (2016). Cryogenic manufacturing processes. CIRP annals, 65(2), 713-736.
Jebaraj, M., & Pradeep Kumar, M. (2019). Effect of cryogenic CO2 and LN2 coolants in milling of aluminum alloy. Materials and Manufacturing Processes, 34(5), 511-520.
Kasim, M. S., Haron, C. C., Ghani, J. A., Sulaiman, M. A., & Yazid, M. Z. A. (2013). Wear mechanism and notch wear location prediction model in ball nose end milling of Inconel 718. Wear, 302(1-2), 1171-1179.
Kaynak, Y., & Gharibi, A. (2018). Progressive tool wear in cryogenic machining: the effect of liquid nitrogen and carbon dioxide. Journal of Manufacturing and Materials Processing, 2(2), 31.
Ke, Y. L., Dong, H. Y., Gang, L. I. U., & Zhang, M. (2009). Use of nitrogen gas in high-speed milling of Ti-6Al-4V. Transactions of Nonferrous Metals Society of China, 19(3), 530-534.
Khare, S. K., & Agarwal, S. (2017). Optimization of machining parameters in turning of AISI 4340 steel under cryogenic condition using Taguchi technique. Procedia CIRP, 63, 610-614.
Satyanarayana Kosaraju, V. G. A., & Popuri, B. B. (2012). Taguchi analysis on cutting forces and temperature in turning titanium Ti-6Al-4V. International Journal of Mechanical and Industrial Engineering (IJMIE), ISSN, (2231-6477), 55-59.
Radzi, M. M., Muhamad, N., Sulong, A. B., Haron, C. H. C., Razak, Z., Akhtar, M. N., ... & Tharazi, I. (2018). Optimization of injection molding parameters: Improving mechanical properties of kenaf reinforced polypropylene composites. Journal of Advanced Manufacturing Technology (JAMT), 12(2), 107-120.
Muhamad, S. S., Ghani, J. A., & Haron, C. H. C. (2018). A review on future implementation of cryogenic machining in manufacturing industry. Progress in Industrial Ecology, an International Journal, 12(3), 260-283.
Muhamad, S. S., Ghani, J. A., Juri, A., & Haron Che, H. C. (2019). Dry and cryogenic milling of AISI 4340 alloy steel. Jurnal Tribologi, 21, 1–12.
Musfirah, A. H., Ghani, J. A., & Haron, C. C. (2017). Tool wear and surface integrity of inconel 718 in dry and cryogenic coolant at high cutting speed. Wear, 376, 125-133.
Natasha, A. R., et al. "Temperature at the Tool Chip Interface in Cryogenic and Dry Turning of AISI 4340 Using Carbide Tool." International Journal of Simulation Modelling 15.2 (2016): 201-212.
Natasha, A. R., Ghani, J. A., Haron, C. C., & Syarif, J. (2018, January). The influence of machining condition and cutting tool wear on surface roughness of AISI 4340 steel. In IOP Conference Series: Materials Science and Engineering (Vol. 290, No. 1, p. 012017). IOP Publishing.
Qasim, A., Nisar, S., Shah, A., Khalid, M. S., & Sheikh, M. A. (2015). Optimization of process parameters for machining of AISI-1045 steel using Taguchi design and ANOVA. Simulation Modelling Practice and Theory, 59, 36-51.
Qian, L., & Hossan, M. R. (2007). Effect on cutting force in turning hardened tool steels with cubic boron nitride inserts. Journal of Materials Processing Technology, 191(1-3), 274-278.
Ravi, S., & Kumar, M. P. (2011). Experimental investigations on cryogenic cooling by liquid nitrogen in the end milling of hardened steel. Cryogenics, 51(9), 509-515.
Sahoo, A. K., & Sahoo, B. (2012). Experimental investigations on machinability aspects in finish hard turning of AISI 4340 steel using uncoated and multilayer coated carbide inserts. Measurement, 45(8), 2153-2165.

Singla, A. K., Singh, J., & Sharma, V. S. (2018). Processing of materials at cryogenic temperature and its implications in manufacturing: A review. Materials and Manufacturing Processes, 33(15), 1603-1640.

Subramanian, M., Sakthivel, M., Sooryaprakash, K., & Sudhakaran, R. (2013). Optimization of cutting parameters for cutting force in shoulder milling of Al7075-T6 using response surface methodology and genetic algorithm. Procedia Engineering, 64, 690-700.

Sumitomo. (2017). Sumitomo High Performance Cutting Tools General Catalog 2017/2018.

Tan, Y. H., Abdullah, M. O., Nolasco-Hipolito, C., & Zauzi, N. S. A. (2017). Application of RSM and Taguchi methods for optimizing the transesterification of waste cooking oil catalyzed by solid ostrich and chicken-eggshell derived CaO. Renewable Energy, 114, 437-447.

Zhong, Z. Q., Zhang, L., Zhou, L., Qiu, L. C., Shi, H. D., Yang, M. L., & Zhu, J. F. (2018). Cutting performances and the related characteristics of CVD coated hardmetal inserts changed by post-treatments. International Journal of Refractory Metals and Hard Materials, 70, 162-168.